Desalination and Water Treatment
www.deswater.com

doi:10.5004/dwt.2019.24080

153 (2019) 208–215
June

Adsorption performance of Pb(II) ions from aqueous solution onto a novel complex of coffee grounds and attapulgite clay

Lu Liu[a], Luji Yu[a], Wei Zhang[a,b,c,d,*], Jiahui Fan[a], Qiting Zuo[a,b,c,*], Mengjia Li[e], Zhenfei Yan[a], Zhangchao You[a], Renyu Wang[a]

[a]*School of Water Conservancy & Environment, Zhengzhou University, 100 Kexue Avenue, Zhengzhou, Henan, 450001, P. R. China*
[b]*Zhengzhou Key Laboratory of Water Resource and Environment, Zhengzhou, 450001, China,*
email: zhangwei88@zzu.edu.cn (W. Zhang), (zuoqt@zzu.edu.cn (Q. Zuo)
[c]*Henan Key Laboratory of Groundwater Pollution Prevention and Rehabilitation, Zhengzhou, 450001, China*
[d]*Henan Province Key Laboratory of Water Pollution Control and Rehabilitation Technology, Pingdingshan, 467036, China*
[e]*School of Materials Science and Engineering, Zhengzhou University, 100 Kexue Avenue, Zhengzhou, Henan, 450001, P. R. China*

Received 11 November 2018; Accepted 5 March 2019

ABSTRACT

As one kind of easily available, low cost and long-duration method, the adsorption method procedure has already been applied widely in water treatment for recent years. In this paper, synthesized complex of coffee grounds and attapulgite clay (CG/AC) was designed through hydrothermal reaction and employed for removal of toxic Pb(II) ions. The adsorbent of designed CG/AC was characterized by means of FTIR, XRD and SEM. The results were indicating that CG was loaded well with AC through preparation by combination of hydrothermal synthesis. The Pb(II) adsorption kinetic was well fitted by second order model from the adsorption kinetic experiments. The adsorption reaction reached equilibrium within 60 min and the maximum adsorption capacity was 4.45 $mg \cdot g^{-1}$at 25°C. The adsorption isotherm for Pb(II) was better fitted by Langmuir isotherm model. The higher temperature would be beneficial to adsorption of Pb(II) by designed CG/AC and the maximum adsorption capacity could reach up to 6.98 $mg \cdot g^{-1}$ at 35°C. Thus, CG/AC showed relatively great potential for adsorption capacity of Pb(II) in aqueous solution, which should shed light on its application in wastewater treatment.

Keywords: Coffee grounds; Attapulgite Clay; Designing complex; Adsorption

1. Introduction

The excessive emission of heavy metals i.e., Pb(II), Cr(VI), Hg(II), Cd(II) into the water environment have already become a major global environmental problem [1].Those mentioned heavy metals were mainly originating from metallurgical mining industry, chemical industry, electroplating industry, landfill leachates and even agricultural nonpoint source pollution [2,3]. Due to its recalcitrance and persistence in the water or related environment, more attention was paid to the removal of heavy metals from the water body [4]. The major source of lead in water originating from effluents of industries, i.e., lead alloys, lead-acid batteries, plastics, solder, tubing and pigments [5,6]. The uncontrolled discharge would inevitably cause adverse effects on ecosystems and accumulation in human body through food chains [7].

A series of methods including chemical precipitation [8], ion-exchange [9,10], membrane filtration [11] and electrochemical treatment approach [12] were investigated to remove heavy metals in water environment. Nevertheless, these above mentioned methods have many disadvantages including their high investment, operating cost and secondary pollution [13].

The adsorption method was considered as an alternative approach for treatment of Pb(II) polluted water due to its effectiveness, lower cost and possible reversibility for recent years [14]. Basically, adsorption method was a mass

---

*Corresponding author.

1944-3994 / 1944-3986

transfer process, where the pollutants would be transferred from the liquid phase to the surface of the solid materials, which was bound by physical and/or chemical interactions. During the adsorption procedure, it was crucial to design a novel adsorbent with appropriate structure, lower cost, easier accessibility and higher adsorption efficiency. Thusly, some novel adsorbents was chosen and applied including agricultural waste [15–17], fruit shells [18], crustaceans [19] and clay minerals [20,21].

As a kind of inexpensive and efficient adsorbents, the clay minerals have relatively higher chemical and mechanical stability, high surface area and ideal structural properties with huge yield, which was mainly consisting of montmorillonite [20], attapulgite [22], kaolin [21] and mica [23]. The attapulgite clay (Abbreviated as, AC) was a crystalline hydrated magnesium silicate with large specific surface area and moderate cation exchange capacity, which was beneficial for the adsorption of heavy metals as reported in the previous study [24]. Nevertheless, the nano rods of AC would naturally aggregate and cause a poor dispersion, which would greatly limit its application in water treatment [25]. Thus, it was crucial to modify the AC material to improve its dispersion characteristic. Here, the AC material would be modified by the coffee grounds (Abbreviated as, CG) for its widely existence and lower cost. It would be a preferable choice if the coffee grounds could combine with the attapulgite clay and form into a novel network structure. What's more, CG was also one kind of adsorbents for treatment of Pb(II) ions polluted water, as reported in previous literatures [26,27]. Thus, the structure and combining model of AC with CG were still needed to be investigated, which would provide a reference for the research of new complex materials.

Thus, CG and AC have been chosen as raw materials for the preparation of adsorbent complex in this study. Adsorbent complex was fabricated by hydrothermal reaction, followed by analyzed through adsorption kinetics and isotherms experiments to study the adsorption characteristics of Pb(II). The adsorption mechanism of Pb(II) by CG/AC was interpreted by analyzing its inner structure.

2. Materials and methods

2.1. Raw materials

Coffee grounds (CG), which was directly collected from Starbucks coffee shop, then followed by washing with deionized water for several times until the impurities were eliminated. The coffee grounds after washing were dried in an oven at a temperature of 80°C until constant weight was reached. Attapulgite clay (AC) with nanometer scale was purchased from Dingbang Minerals Technology Co., Ltd. (Changzhou, Jiangsu, China). Both raw materials of CG and AC were stored for further analyses.

2.2. Characterization methods

The morphologies of CG, AC and CG/AC were all observed on a Scanning electron microscope (SEM) (Zeiss Auriga, Germany). The Fourier transform infrared (FTIR) (VERTEX 70, Bruker, Germany) and powder X-ray diffraction (XRD) (Philips, PANalytical B.V., Holland) were applied to analyze the phase composition of the complex. The X-ray diffraction (XRD) analysis was carried out with X-ray diffractometer. Patterns were recorded from 5° to 80° 2θ at a scan rate 1° min^{-1}. The FTIR of CG, AC and CG/AC were all recorded in the range of 4000~400 cm^{-1}.

2.3. Preparation of CG/AC complex

The CG/AC complex was prepared by the following stages: (1) 3.0 g of AC was suspended in 100 mL hydrochloric acid (concentration of 3 mol·L^{-1}) until the AC was dissolved. (2) 3.0 g of CG was gradually added into the suspension, followed by sealed and reacted for 8 h at 70°C by using thermostat water bath. (3) At the terminal of the reaction, CG/AC complex was centrifugal separated and washed by deionized water for several times until the supernatant was neutral. (4) Finally, the CG/AC samples were dried in an oven at 120°C. The obtained CG/AC samples were collected in the desiccator for further treatment. The possible synthetic process of CG/AC complex could be proposed in Fig. 1c.

2.4. Preparation of the Pb(II) solution

The stock solution of Pb(II) solution of 1000 mg·L^{-1} was obtained by dissolving 1.599 g of lead nitrate (chemical formula of $Pb(NO_3)_2$) into 1 L deionized water. The stock solution was then diluted with deionized water to get the planned concentration. The pH of solution was adjusted to 5.5~6.0 by using a solution of HNO_3 or NaOH. The concentrations of Pb(II) for aqueous solution before and after adsorption experiment were detected by using an Inductively coupled plasma-optical emission spectrometer (ICP-OES, Agilent 5100, Australia).

2.5. Pb(II) adsorption experiments

2.5.1. Adsorption kinetics

Two kinds of kinetic models (pseudo-first order and pseudo-second order models) were applied to study the kinetics of adsorption experiment. The parameter of contact time was ranging from 15 to 100 min at 25°C.

The pseudo-first order model was used to fit the experimental data, which could be expressed as the following Eq. (1).

$$\ln(q_e - q_t) = \ln q_e - k_1 t \qquad (1)$$

The pseudo-second order model was used to study the adsorption process and provide insights into possible reaction mechanisms, which could be expressed as Eq. (2).

$$t/q_t = 1/(k_2 q_e^{\,2}) + t/q_e \qquad (2)$$

where q_e (mg·g^{-1}) and q_t (mg·g^{-1}) were the amount of adsorbent adsorbed at equilibrium and any time, respectively. The k_1, $k_2$were the velocity constant of the pseudo-first order and the pseudo-second order.

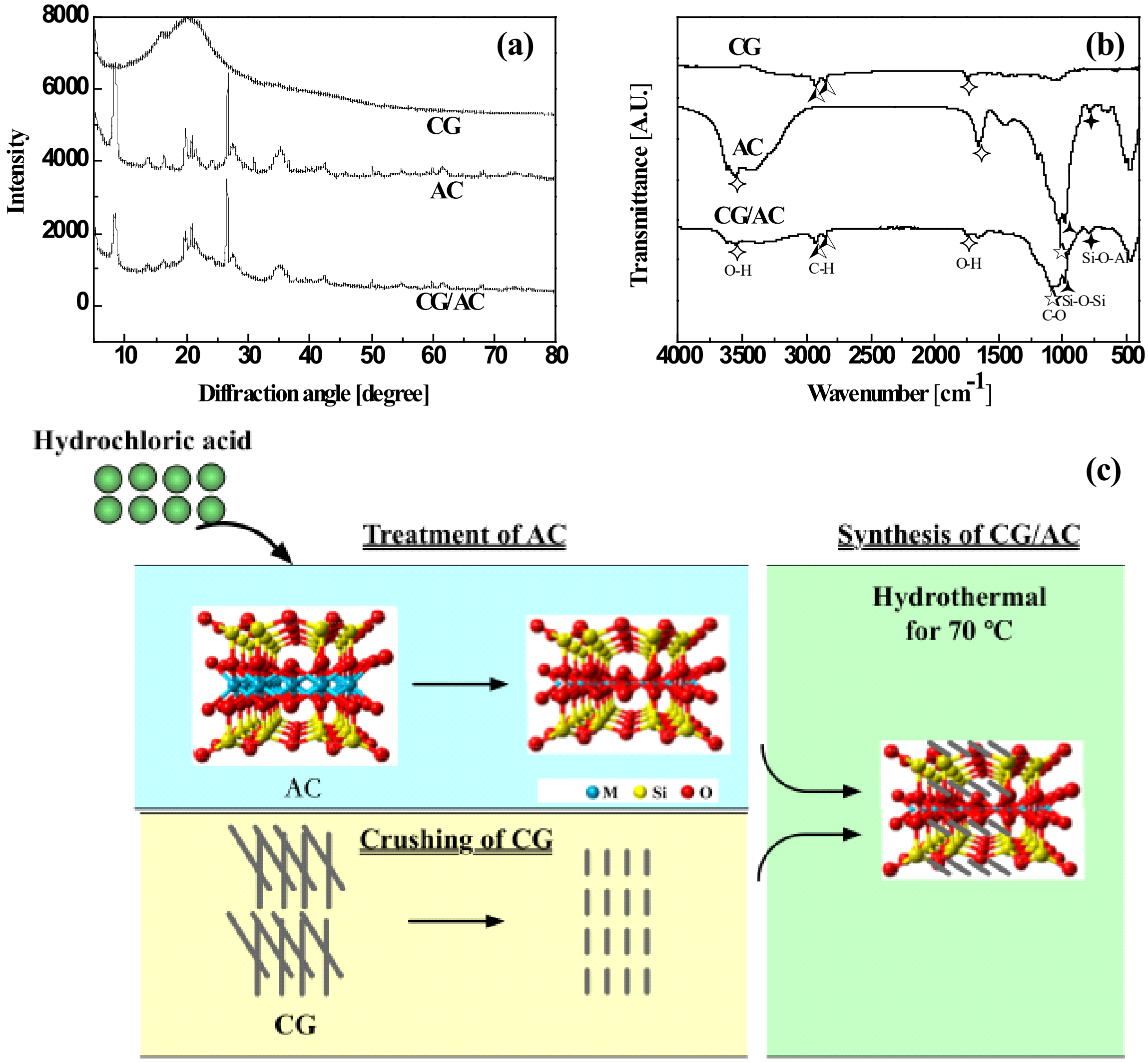

Fig. 1. XRD patterns (a) and FTIR spectra (b) for coffee grounds (CG), attapulgite clay (AC) and the complex of coffee grounds and attapulgite clay (CG/AC) prepared at the temperature of 70°C by hydrothermal reaction for 8 h; (c) The proposed synthesis model of CG/AC containing of treatment of AC by hydrochloric acid and crushing of CG followed by hydrothermal reaction.

2.5.2. Adsorption isotherms

The isotherms of adsorption were studied by using two different isotherm models, which were Langmuir and Freundlich models, respectively. Those models could be applied to determine the proper isotherm for Pb(II) ions adsorbed on CG/AC complex.

The models of Langmuir and Freundlich were expressed by using Eq. (3) and Eq. (4), respectively.

$$\text{Langmuir: } q_e = q_m K_L c_e / (1 + K_L c_e) \quad (3)$$

$$\text{Freundlich: } q_e = K_F {c_e}^{1/n} \quad (4)$$

where q_e (mg·g^{-1}) was the amount of adsorbent adsorbed, q_m (mg·g^{-1}) was the maximum adsorption capacity, c_e (mg·g^{-1}) was the equilibrium solute concentration, K_L (L·mg^{-1}) was the Langmuir constant related to adsorption energy, K_F and n were Freundlich constants and intensity factors, respectively.

3. Results and discussion

3.1. Characterization of prepared CG/AC complex

The XRD patterns for the raw materials and CG/AC complex are shown in Fig. 1a. The main characteristic peaks at d of 10.39, 4.44, 2.53 and 1.50 for CG/AC were indicating the presence of $Mg_5Si_8O_{20}(OH)_2(OH_2)_4{\cdot}4H_2O$ phase, indicating AC was included in the complex. These peaks (d = 4.44, d = 4.25, d = 4.36 and d = 1.82) of CG/AC left shifted compared with AC, while the characteristic peaks of CG were not observed in the XRD patterns, indicating that CG did not intercalate the crystal layers of AC. CG was probably adsorbed in surface of the micro/nano pores and nano channels of AC. Additionally, some characteristic peaks (d = 10.39, d = 4.44, d = 4.25 and d = 3.36) of AC in CG/AC's XRD patterns became weakened compared with AC alone, illustrating the higher dispersion of CG/AC samples, which was in accordance with the result of SEM in Fig. 2.

The FTIR analysis results are shown in Fig. 1b. As shown in Fig. 1b, the prepared CG/AC possessed the characteristic peaks of CG (2926 cm^{-1} and 2855 cm^{-1} for C-H stretching vibration) and AC (986 cm^{-1} for Si-O-Si stretching vibration, 799 cm^{-1} for Si-O-Al stretching vibration), indicating that CG was successfully combined with AC. The bands observed at 3551 cm^{-1} and 1658 cm^{-1} were assigned to the stretching of O-H group. The bands at 2926 cm^{-1} and 2855 cm^{-1} illustrated the asymmetric and symmetric C-H stretching vibration, respectively. The strength of peak of CG/AC (1088 cm^{-1} for stretching vibration of C-O and 799 cm^{-1} for stretching vibration of Si-O-Al) weakened and the peak (3551 cm^{-1} and 986 cm^{-1} for stretching vibration of O-H) intensified compared with the raw materials [28–32]. Additionally, not any new peaks were observed in the prepared CG/AC, indicating that no obvious chemical reactions were conducted during the preparation process of CG/AC.

The morphology images of CG, AC and CG/AC are shown in Fig. 2. As shown in Fig. 2, the CG had a relatively smooth surface and specific porous structure (Figs. 2a,b), while the AC would tend to aggregate and form into compact bunches (Fig. 2c). From the appearance of prepared CG/AC (Fig. 2d), the compact bunches of AC became obviously loose in the CG/AC, while the AC was loaded well with CG after hydrothermal reaction. The results were indicating that the hydrothermal reaction procedure would affect the agglomeration of AC. The formation of complex networks could significantly improve the dispersion of AC, while more Pb(II) ions could be retained in the micro networks. The EDS mapping for C, Si and O elements of the complex is shown in Fig. 2e, while the EDS spectra is shown in Fig. 2f. The element distribution results were indicating that Si and O were obvious dominant elements, accompanying C. The existence of C in the EDS mapping results were also indicating that the AC were loaded well with CG.

3.2. Adsorption kinetics

The effect of contact time on adsorption rate of Pb(II) by CG/AC is displayed in Fig. 3a. As shown in Fig. 3a, the removal rate of Pb(II) was increasing rapid at the initial stage of 0~40 min, which was in accordance with previous studies [33,34]. Subsequently, the adsorption rate gradu-

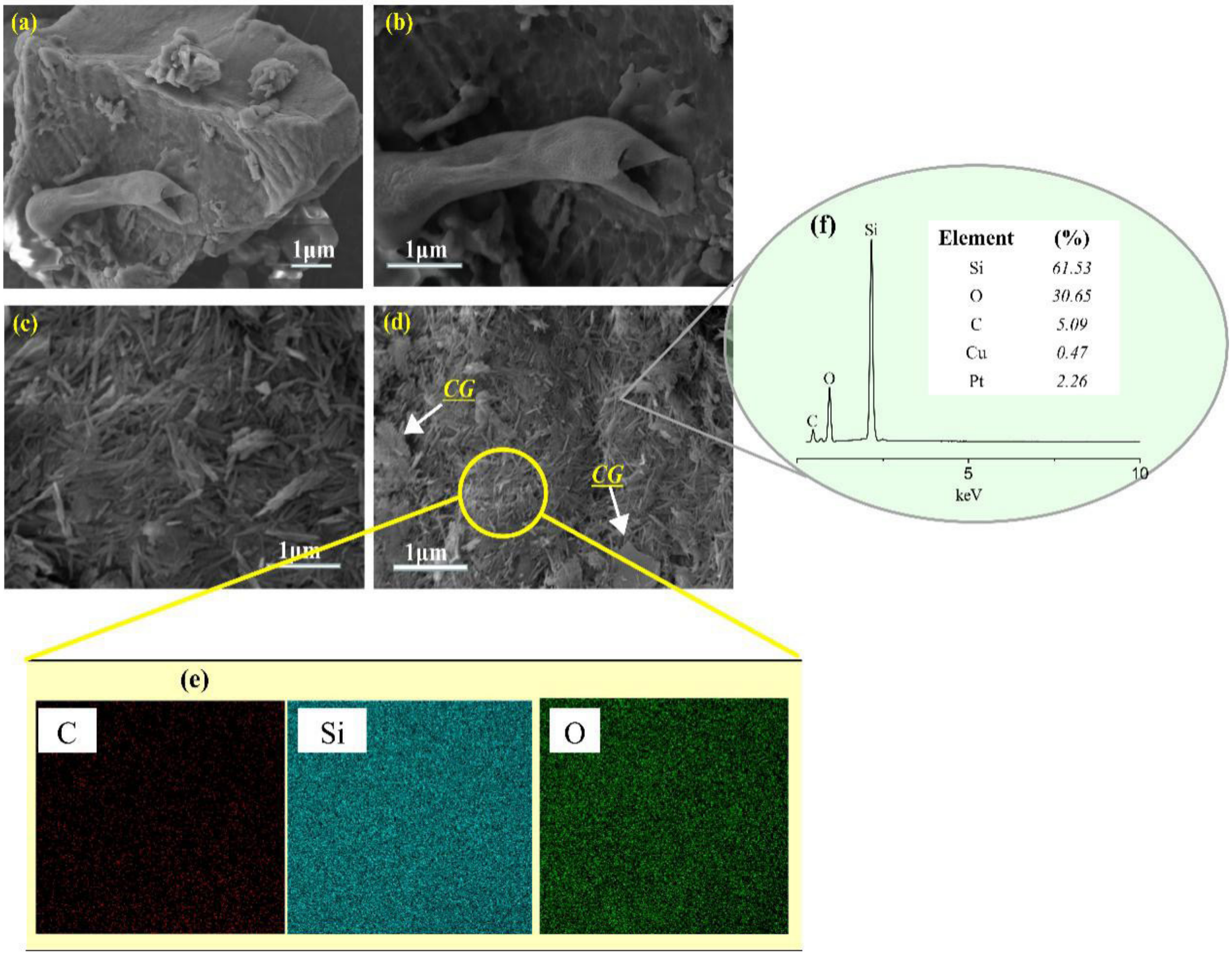

Element	(%)
Si	61.53
O	30.65
C	5.09
Cu	0.47
Pt	2.26

Fig. 2. SEM images of original coffee ground (a), (b), the original attapulgite clay (c), the complex of coffee grounds and attapulgite clay (d); EDS mapping for C, Si and O elements of the complex; (f) EDS spectra for the complex.

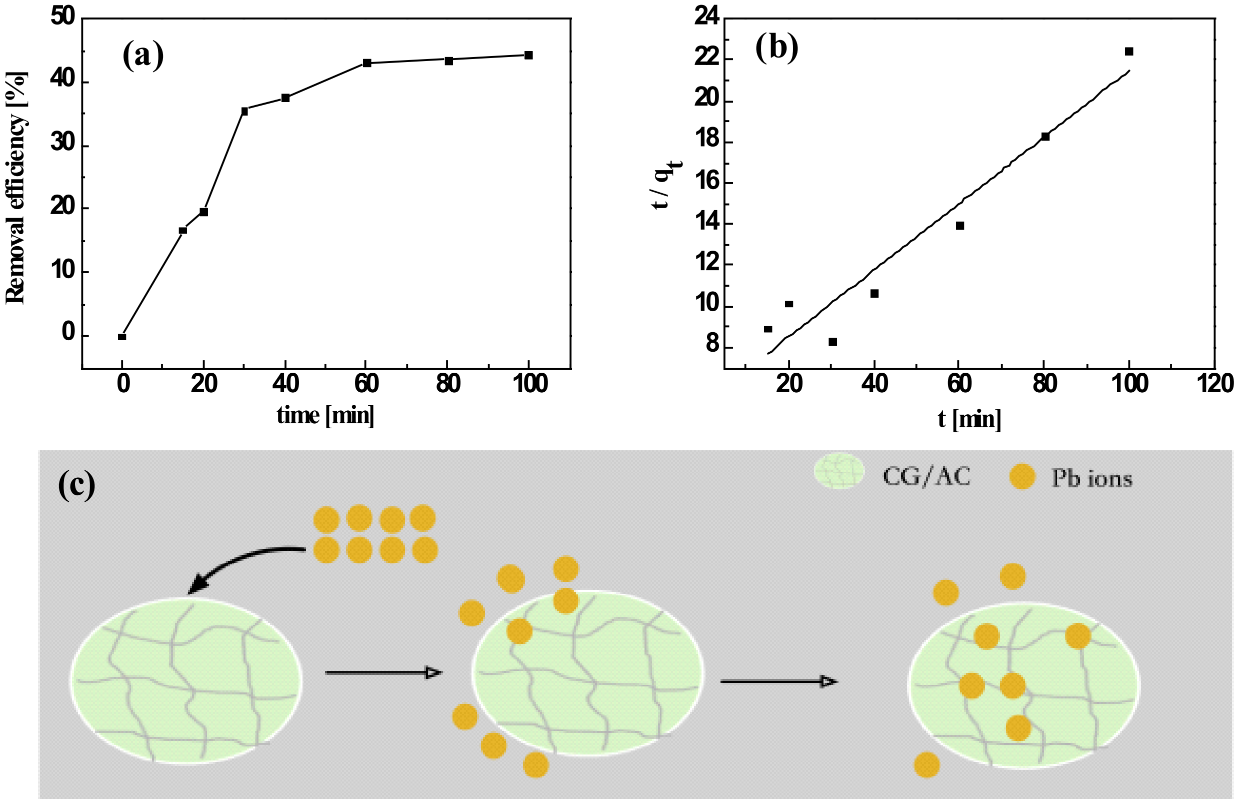

Fig. 3. Effect of contact time on the rate of adsorption (a) at condition: temperature of 25°C, pH of 5.5~6.0, adsorbent dosage of 0.1 g and $[Pb(II)]_0$ of 50 mg·L^{-1}; Pseudo-second order kinetic equation fitting curve (b); The schematic diagram (c) of CG/AC adsorbing Pb(II) ions in aqueous solution.

ally slowed down and the equilibrium time was about 100 min. Generally, the adsorption progress of Pb(II) by CG/AC could be divided into two stages: fast reaction and slow reaction. In the fast reaction stage, Pb(II) were adsorbed on the surface of the adsorbents, where the adsorption rate was mainly depended on the diffusion of Pb(II) and the equilibrium could be achieved in a short time. In the slow reaction stage, Pb(II) would gradually entered into the inner surface of the adsorbents. The reaction rate was affected by surface structure of adsorbents, initial concentration of metal ions of solution [1]. It was confirmed that Pb(II) element was determined in the CG/AC complex after adsorption process according to the EDS analysis (Figs. 4a, b), demonstrating the adherence of Pb(II) ions on CG/AC surface.

The kinetic rate constants are shown in Table 1, which were obtained from first order and second order pseudo-kinetic models. The results were indicating that the adsorption processes of Pb(II) by CG/AC were matched well with the pseudo-second-order kinetic model and the model fit is presented in Fig. 3b. As the proposed adsorption model shown in Fig. 3c, the adsorption mechanism could be expressed by three steps [35,36]. Firstly, the Pb(II) ions would be transferred from bulk solution to CG/AC surface across the liquid film surrounding the adsorbent particle (External diffusion) [37]. Secondly, Pb(II) ions would be diffused inside the internal structure of CG/AC particle (Intraparticle diffusion) [38]. Finally, Pb(II) ions would be absorbed at interior sites.

3.3. Adsorption isotherms

The corresponding values of Langmuir and Freundlich isotherms were calculated and represented in Table 2. It was observed that the Langmuir isotherm would better described the adsorption of Pb(II) for its higher correlation coefficient R^2. It was assumed that the adsorbed Pb(II) would form into monolayer coverage on the surface of absorbents, which was containing finite number of identical sorption sites [39]. The isotherm profiles of Pb(II) adsorption at various temperatures (25°C, 30°C and 35°C) are shown in Figs. 5a–c. It was obvious that the adsorption value gradually boosted strength, then leveled off until saturation. The maximum adsorption capacity of Pb(II) was observed as 6.98 mg·g^{-1}. The removal of Pb^{2+} increased from 62% to 97.5% for 25–45°C, indicating that the higher temperature was beneficial to adsorption of Pb(II) by adsorbent. The proposed model can be expressed by Fig. 5d, thereby indicating the endothermic nature of Pb(II) ions onto CG/AC [34,40,41,42]. The FTIR spectra after adsorption are shown in Fig. 6. It is apparent that the position of all the valence bonds were not changed after adsorption, which could be interpreted that the amount of CG/AC complex was far greater than the amount of Pb(II) absorbed.

The aim of this paper was to study the properties of the complex, which was made from two raw materials with different structural characteristics. The adsorption properties of the complex were explored through a large number of experiments. Compared with other adsorp-

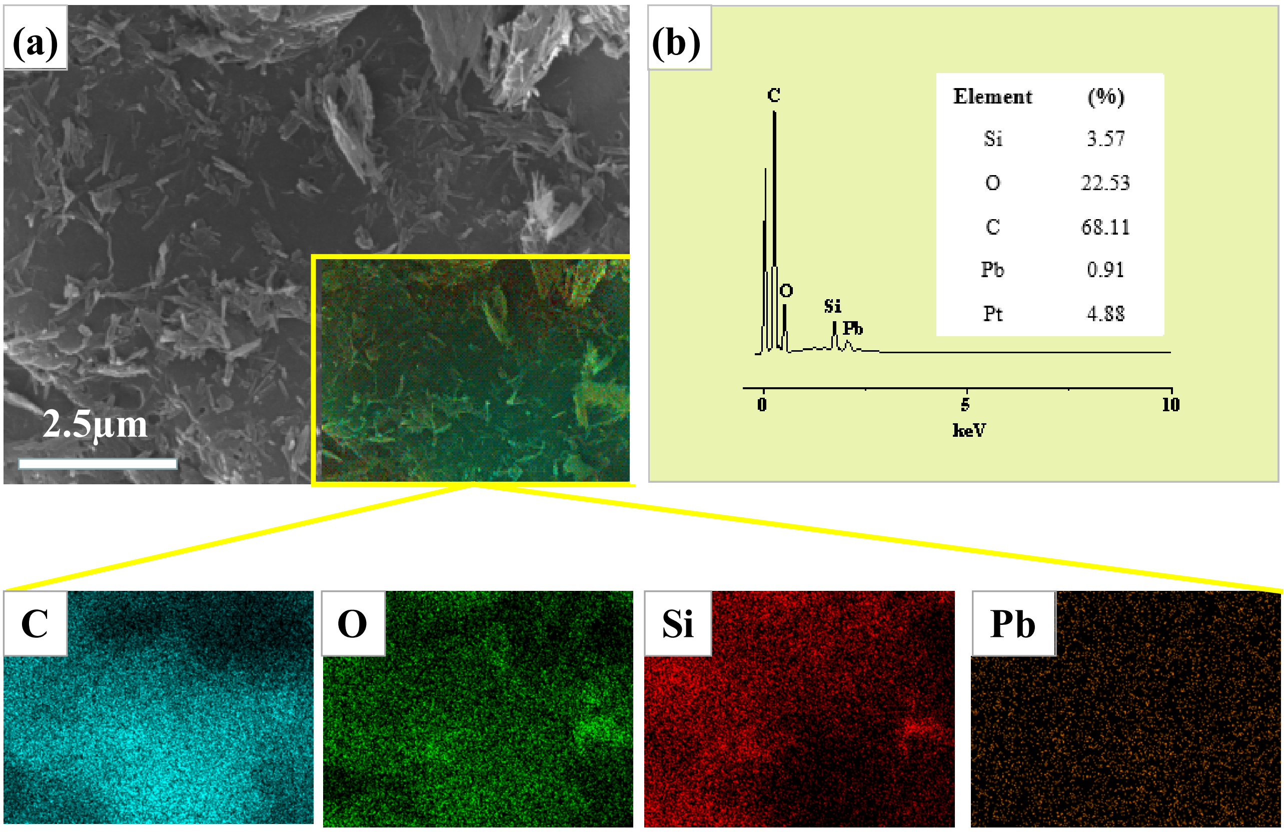

Fig. 4. SEM image, EDS mapping (a) and EDS spectra (b) of CG/AC complex after Pb(II) ions adsorption at condition: temperature of 25°C, pH of 5.5~6.0, adsorbent dosage of 0.1 g and $[Pb(II)]_0$ of 200 mg·L^{-1}.

Table 1
Kinetic constants for lead adsorption onto CG/AC

Sample	Pseudo-first order model			Pseudo-second order model		
	q_e (mg·g^{-1})	k_1 (min^{-1})	R^2	q_e (mg·g^{-1})	K_2 (g·mg^{-1}·min^{-1})	R^2
CG/AC	4.72	0.035	0.91275	6.19	0.00493	0.9374

Table 2
Isotherm constants for lead adsorption onto CG/AC

Sample	Temperature	Langmuir			Freundlich		
		q_m (mg·g^{-1})	K_L (L·mg^{-1})	R^2	K_F (L·mg^{-1})	$1/n$ (g·L^{-1})	R^2
CG-AC	25°C	6.50	0.0595	0.88831	1.8294	0.2394	0.76544
	30°C	7.71	0.0452	0.82788	1.6643	0.5838	0.70773
	35°C	8.68	0.0490	0.83374	1.9286	0.2880	0.69683

tion materials reported in related literature, the adsorption capacity was not ideal. Its adsorption capacity might be further improved by modification or other methods.

4. Conclusions

This work designed and synthesized a novel adsorbent of CG/AC to removal Pb(II) from aqueous solution, resulting in improving the adsorption performance of Pb(II). The kinetic experiment showed that the adsorption rate was rapid and maximum adsorption capacities was achieved at 100 min. The adsorption of Pb(II) fitted the pseudo-second-order kinetic model well. For all the temperatures studied, Langmuir isotherm model was in good accordance with the experimental data compared with Freundlich. In conclusion, CG/AC might be an effective candidate for environmental protection, for its removal of Pb(II) from aqueous solution.

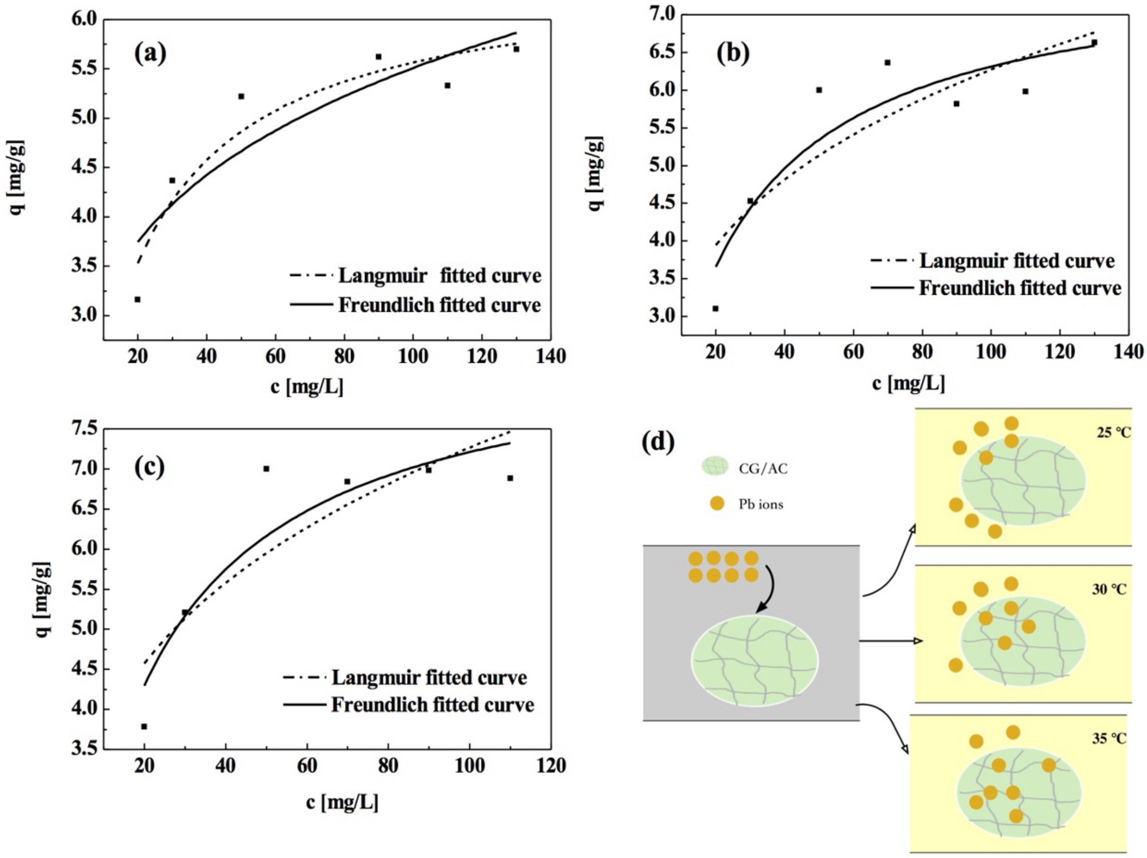

Fig. 5. Adjusted isotherms for adsorption of Pb(II) ions with CG/AC for various temperature conditions: T = 25°C (a); T = 30°C (b); T = 35°C (c). Other conditions: pH of 5.5~6.0, adsorbent dosage of 0.1 g. (d) presents for proposed adsorption procedure of CG/AC at various temperatures.

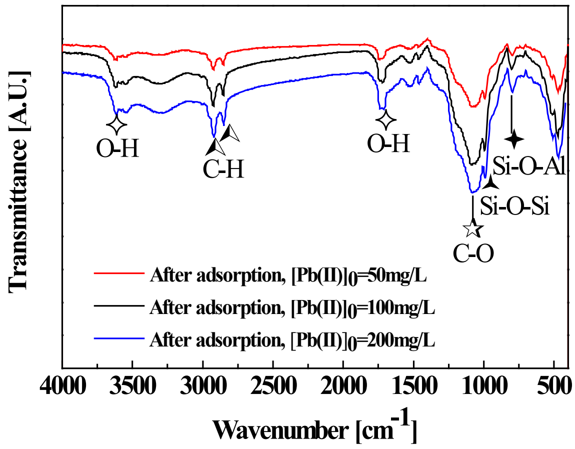

Fig. 6. FTIR spectra of CG/AC after Pb(II) ions adsorption at condition: temperature of 25°C, pH of 5.5~6.0, adsorbent dosage of 0.1 g and $[Pb(II)]_0$ of 50 mg·L^{-1}, 100 mg·L^{-1}, 200 mg·L^{-1}, respectively.

Acknowledgement

The authors would like to express their thanks to the fund supported by China Postdoctoral Science Foundation (2018M632799), National Science and Technology Major Project for Water Pollution Control and Treatment (2015ZX07204-002), Education Department of Henan Province Science Research Program (18B610008, 19A610010),Key research and development and promotion special (182102311033). The authors would also thank Key Project of Natural Science Foundation of China - Xinjiang Joint Fund (No. U1803241) and The Natural Sciences Foundation of China (No. 51779230). Also, the authors would also express they're thanks to the Modern Analysis and Computing Center of Zhengzhou University for various materials analysis offered.

References

[1] N. Azouaou, Z. Sadaoui, A. Djaafri, H. Mokaddem, Adsorption of cadmium from aqueous solution onto untreated coffee grounds: equilibrium, kinetics and thermodynamics, J. Hazard. Mater., 184 (2010) 126–134.

[2] D. Ko, J.S. Lee, H.A. Patel, M.H. Jakobsen, Y. Hwang, C.T. Yavuz, H.C.B Hansen, H.R. Andersen, Selective removal of heavy metal ions by disulfide linked polymer networks, J. Hazard. Mater., 332 (2017) 140–148.

[3] F. Zhang, Y. Li, M. Yang, W. Li, Content of heavy metals in animal feeds and manures from farms of different scales in northeast China, Int. J. Environ. Res. Public. Heal. Th., 9 (2012) 2658–2668.

[4] F. Fu, Q. Wang, Removal of heavy metal ions from wastewaters: a review, J. Environ. Manage., 92 (2011) 407–418.

[5] P.A. Kobielska, A.J. Howarth, O.K. Farha, S. Nayak, Metal–organic frameworks for heavy metal removal from water, Coord. Chem Rev., 358 (2018) 92–107.

[6] T. Tatarchuk, M. Bououdina, B. Al-Najar, R.B. Bitra, Green and Ecofriendly Materials for the Remediation of Inorganic and Organic Pollutants in Water, Springer, Cham., 2019, pp. 69–110.

[7] R. Naseem, S.S. Tahir, Removal of Pb(ii) from aqueous/acidic solutions by using bentonite as an adsorbent, Water Res., 35 (2001) 3982–3986.

[8] J. Khosravi, A. Alamdari, Copper removal from oil-field brine by coprecipitation, J. Hazard. Mater., 166 (2009) 695–700.

[9] A. Górka, J. Zamorska, D. Antos, Coupling ion exchange and biosorption for copper(II) removal from wastewaters, Ind. Eng. Chem. Res., 50 (2011) 3494–3502.

[10] M. Naushad, Z.A. Alothman, Separation of toxic Pb^{2+}, metal from aqueous solution using strongly acidic cation-exchange resin: analytical applications for the removal of metal ions from pharmaceutical formulation, Desal. Water Treat., 53 (2015) 2158–2166.

[11] B. Aftab, S.J. Khan, T. Maqbool, N.P. Hankins, Heavy metals removal by osmotic membrane bioreactor (OMBR) and their effect on sludge properties, Desalination, 403(2017) 117–127.

[12] M.A. Barakat, New trends in removing heavy metals from industrial wastewater,Arab J. Chem., 4 (2011) 361–377.

[13] H. Lin, Y. Yang, Y.B. Dong, Influence factors of adsorbent material dealing with Zn^{2+}, J. Mater. Met., (2012).

[14] I.F. Mironyuk, V.M. Gun'ko, H.V. Vasylyeva, O.V. Goncharuk, T.R. Tatarchuk, V.I. Mandzyuk, N.A. Bezruka, T.V. Dmytrotsa, Effects of enhanced clusterization of water at a surface of partially silylated nanosilica on adsorption of cations and anions from aqueous media, Micropor. Mesopor. Mater., 277 (2019) 95–104.

[15] S. Nethaji, A. Sivasamy, A.B. Mandal, Preparation and characterization of corn cob activated carbon coated with nano-sized magnetite particles for the removal of Cr (VI), Bioresour. Technol., 134 (2013) 94–100.

[16] M. Ghasemi, M. Naushad, N. Ghasemi, Y. Khosravi-fard, Adsorption of Pb(II) from aqueous solution using new adsorbents prepared from agricultural waste: adsorption isotherm and kinetic studies, J. Ind. Eng. Chem., 20 (2014) 2193–2199.

[17] M. Ghasemi, M. Naushad, N. Ghasemi, Y. Khosravi-fard, A novel agricultural waste based adsorbent for the removal of Pb(II) from aqueous solution: Kinetics, equilibrium and thermodynamic studies, J. Ind. Eng. Chem., 20 (2014) 454–461.

[18] F.V. Pereira, L.V. Gurgel, L.F. Gil, Removal of Zn^{2+} from aqueous single metal solutions and electroplating wastewater with wood sawdust and sugarcane bagasse modified with EDTA dianhydride (EDTAD), J. Hazard. Mater., 176 (2010) 856–863.

[19] S. Dahiya, R.M. Tripathi, A.G. Hegde, Biosorption of lead and copper from aqueous solutions by pre-treated crab and arca shell biomass, Bioresour. Technol., 99 (2008) 179–187.

[20] D.A. Almasri, T. Rhadfi, M.A. Atieh, G. Mckay, S. Ahzi, High performance hydroxyiron modified montmorillonite nanoclay adsorbent for arsenite removal, Chem. Eng. J., 335 (2017).

[21] L. Mouni, L. Belkhiri, J.C. Bollinger, A. Bouzaza, A. Assadi, A. Tirri, F. Dahmoune, K. Madani, H. Remini, Removal of Methylene Blue from aqueous solutions by adsorption on kaolin: Kinetic and equilibrium studies, Appl. Clay Sci., 153 (2017) 38–45.

[22] W. Bigui, Z. Xiaofei, C. Xiabing, Facile preparation of magnetic graphene oxide and attapulgite composite adsorbent for the adsorption of Ni(II), IOP Conf Ser: Earth Environ. Sci., 104 (2017) 012019.

[23] R. Ahmad, A. Mirza, Application of xanthan gum/ n-acetyl cysteine modified mica bionanocomposite as an adsorbent for the removal of toxic heavy metals, Groundwater Sustain Dev., (2018).

[24] H. Chen, A. Wang, Adsorption characteristics of Cu (II) from aqueous solution onto poly(acrylamide)/attapulgite composite, J. Hazard. Mater., 165 (2009) 223–231.

[25] L. He, M. Wang, G. Zhang, G. Qiu, D. Cai, Z. Wu, X. Zhang, Remediation of Cr (VI) contaminated soil using long-duration sodium thiosulfate supported by micro-nano networks, J. Hazard. Mater., 294 (2015) 64–69.

[26] X. Ma, F. Ouyang, Adsorption properties of biomass-based activated carbon prepared with spent coffee grounds and pomelo skin by phosphoric acid activation, Appl. Surf. Sci., 268 (2013) 566–570.

[27] L.F. Ballesteros, J.A. Teixeira, S.I. Mussatto, Chemical, functional, and structural properties of spent coffee grounds and coffee silverskin, Food Bioprocess. Technol., 7 (2014) 3493–3503.

[28] T.R. Tatarchuk, M. Bououdina, N.D. Paliychuk, I.P. Yaremiy, V.V. Moklyak, Structural characterization and antistructure modeling of cobalt-substituted zinc ferrites, J. Alloy Comp., 694 (2017) 777–791.

[29] T.R. Tatarchuk, N.D. Paliychuk, M. Bououdina, B. Al-Najar, M. Pacia, W. Macyk, A. Shyichuk, Effect of cobalt substitution on structural, elastic, magnetic and optical properties of zinc ferrite nanoparticles, J. Alloy Comp., 731 (2018) 1256–1266.

[30] O.I.H. Dimitry, Z. Abdeen, E.A. Ismail, A.L.G. Saad, Studies of particle dispersion in elastomeric polyurethane/organically modified montmorillonite nanocomposites, Int. J. Green Nanotechnol., 3 (2011) 197–212.

[31] U.M. Lathiya, H.O. Jethva, M.J. Joshi, P.M. Vyas, Powder XRD, TEM, FTIR and thermal studies of strontium tartrate nanoparticles, AIP Conf Proc., 2017.

[32] B.R. Babu, T. Tatarchuk, Elastic properties and antistructural modeling for nickel-zinc ferrite-aluminates, Mater. Chem. Phys., 207 (2018) 534–541.

[33] M. Naushad, Surfactant assisted nano-composite cation exchanger: development, characterization and applications for the removal of toxic Pb^{2+} from aqueous medium, Chem. Eng. J., 235 (2014) 100–108.

[34] A. Mittal, M. Naushad, G. Sharma, Z.A. ALothman, S.M. Wabaidur, M. Alam, Fabrication of MWCNTs/ThO_2 nanocomposite and its adsorption behavior for the removal of Pb(II) metal from aqueous medium, Desal. Water Treat., 57 (2016) 21863–21869.

[35] H. Sharififard, M. Soleimani, Modeling and experimental study of vanadium adsorption by iron-nanoparticle-impregnated activated carbon, Res. Chem. Intermed., 43 (2017) 2501–2516.

[36] T.S.Y. Choong, T.N. Wong, T.G. Chuah, A. Idris, Film-pore-concentration-dependent surface diffusion model for the adsorption of dye onto palm kernel shell activated carbon, J. Colloid. Interf. Sci., 301 (2016) 436–440.

[37] W. Shi, Z. Wang, Y.Q. Fu, Enhancement of adsorption and diffusion of lithium in single-walled carbon nanotubes by external electric field, J. Nanopart. Res., 18 (2016) 325.

[38] T. Sato, K. Nakatani, Analysis of distribution and intraparticle diffusion of a fluorescent dye in mesoporous silica gel by confocal fluorescence microspectroscopy, Anal. Sci., 33 (2017) 179–183.

[39] M.R. Abukhadra, F.M. Dardir, M. Shaban, E.A. Ahmed, M.F. Soliman, Superior removal of Co^{2+}, Cu^{2+}, and Zn^{2+}contaminants from water utilizing spongy Ni/Fe carbonate–fluorapatite; preparation, application and mechanism, Ecotoxicol. Environ. Safety, 157 (2018) 358–368.

[40] M. Naushad, Z.A. Alothman, M.R. Awual, M.M. Alam, G.E. Eldesoky, Adsorption kinetics, isotherms, and thermodynamic studies for the adsorption of Pb^{2+}, and Hg^{2+}, metal ions from aqueous medium using Ti(IV) iodovanadate cation exchanger, Ionics, 21 (2015) 2237–2245.

[41] A. Pugazhendhi, G.M. Boovaragamoorthy, K. Ranganathan, M. Naushad, T. Kaliannan, New insight into effective biosorption of lead from aqueous solution using Ralstonia solanacearum: characterization and mechanism studies, J. Clean Prod., 174 (2018) 1234–1239.

[42] X. Zhou, C. Wang, C. Fang, R. Yu, Y. Li, W. Lei, Structure and thermal properties of various alcoholysis products from waste poly(ethylene terephthalate), Waste Manage., 85 (2019) 164–174.